

Amorphous Phase Formation and Heat Treating Evolution in Mechanically Alloyed Al-Ti Powders

P. Urban^{1, a}, E.S. Caballero^{1, b}, F. Ternero^{1, c}, F.J.V. Reina^{1, d}, F.G. Cuevas^{2, e}

¹ETS Ingeniería. Univ. Sevilla. Camino de los Descubrimientos s/n. 41092. Sevilla, Spain.

²ETS Ingeniería. Univ. Huelva. Avda. 3 de Marzo s/n, 21071. Huelva, Spain.

^apurban@us.es, ^besanchez3@us.es, ^cfternero@us.es, ^dfrjune10@gmail.com, ^efgcuevas@dqcm.uhu.es

Keywords: aluminium, titanium, mechanical alloying, amorphization.

Abstract. This paper focuses on the microstructural characterization of Al₂₅Ti₇₅, Al₃₇Ti₆₃, Al₅₀Ti₅₀, Al₆₃Ti₃₇ and Al₇₅Ti₂₅ powders mixtures prepared by mechanical alloying (MA). The high-energy ball-milling, up to 75 h, of aluminium and titanium powders leads to a nanocrystalline or an amorphous structure. It is showed that a stable amorphous Al–Ti phase with uniform elemental distribution forms after 50 h of milling in Al₅₀Ti₅₀ alloy. Heat treatment of the different alloys leads to the crystallization of AlTi₃, AlTi, Al₂Ti and Al₃Ti intermetallic compounds. A comprehensive study by laser granulometry, X-ray diffraction (XRD), scanning electron microscopy (SEM), transmission electron microscopy (TEM) and differential scanning calorimetry (DSC) was carried out on the structure, surface morphology and thermal behaviour of the MA Al-Ti mixtures, both of milled and heat treated powders.

Introduction

Amorphous metallic alloys were discovered in 1960 by Klement et al. [1] and can be obtained in a large number of systems by rapid solidification [2] or mechanical alloying [3].

Mechanical alloying (MA) is a solid-state powder process of repeated cold welding, fragmentation, deformation, rewelding and short-range diffusion, in a layer of powder particles trapped between two colliding balls. MA is able to synthesize a variety of equilibrium and non-equilibrium alloys.

Al-Ti alloys are used in automotive and aerospace applications as excellent engineering materials due to their high specific strength and stiffness, high strength retention and high creep resistance at high temperature [4, 5]. However, the poor ductility and high chemical reactivity of Al-Ti alloys are the main factors limiting the industrial-scale production [6-8]. Amorphized Al-Ti alloys was found for a wide range of compositions between 25 and 90at% of titanium and MA time between 15 and 200 hours [9, 15]. The better properties of these systems can be of great interest to many applications.

Experimental Procedure

Pure elemental powders of Al and Ti were mixed to give the desired composition of Al₂₅Ti₇₅, Al₃₇Ti₆₃, Al₅₀Ti₅₀, Al₆₃Ti₃₇ and Al₇₅Ti₂₅. The mixes with 1.5wt.% of wax were then milled up to 75 hours in a high energy attritor ball mill under a purified argon atmosphere. The ball-to-powder weight ratio was controlled to be 50:1. The rotor speed was 500 rpm. The dry ball-milling was carried out at ambient temperature. The MA experiments were interrupted at desired intervals and a small amount of the ball-milled powder was taken out from the vial for analysis. Mean powder particle size and granulometric curves were obtained by laser diffraction. The structure and amorphization progress of the ball-milled powders were characterized by means of XRD, SEM and TEM. Crystallization behavior was studied in a DSC up to a maximum temperature of 600 °C.

Results and Discussion

Granulometry. First, it is determined the relationship between particle size of all the alloys and milling duration. During the first minutes of milling, particle size increases by cold welding, probably because pure aluminum and titanium particles are relatively soft. Then, during the first hour of milling, particles increasingly harden, mainly by work hardening and solid solution strengthening. Therefore, cold welding of soft particles loses importance against fragmentation of more fragile particles. After the first hour of milling particles fragmentation predominates over cold welding. As shown in Fig. 1, particle size of $\text{Al}_{37}\text{Ti}_{63}$ powder milled for 1 hour is about $21.1\ \mu\text{m}$, a little less than as-mixed powder, with $31.8\ \mu\text{m}$. After 5 hours of milling, particle size decreases considerably down to about $4.9\ \mu\text{m}$, because of continuous fracture processes. This behavior of continued fragmentation continues for 12, 25 and 50 hours of milling, with particle sizes about 3.9 , 2.7 and $1.5\ \mu\text{m}$, respectively. After 25 hours of milling, a second peak clearly appears in granulometric curves, with particles of about $30\ \mu\text{m}$. These particles do not really have so big sizes, but the peak is probably due to small particles agglomerated to each other, as later shown by SEM.

Fig. 2 shows mean values of particle size distribution for all Al-Ti alloys. The $\text{Al}_{25}\text{Ti}_{75}$, $\text{Al}_{37}\text{Ti}_{63}$, $\text{Al}_{63}\text{Ti}_{37}$ and $\text{Al}_{75}\text{Ti}_{25}$ alloys have very similar behavior. As-mixed powders have a mean particle size directly proportional to the amount of Al and Ti in the mixture. After 12 hours of milling, particles size decreases from $27.4\ \mu\text{m}$ and $61.8\ \mu\text{m}$ to $4\ \mu\text{m}$ and $7\ \mu\text{m}$ for $\text{Al}_{25}\text{Ti}_{75}$ and $\text{Al}_{75}\text{Ti}_{25}$, respectively. Between 12 and 75 hours of milling there is little difference in particle size. In contrast, the $\text{Al}_{50}\text{Ti}_{50}$ alloy needs to be milled up to 50 hours to obtain a particle size similar to that in the other alloys.

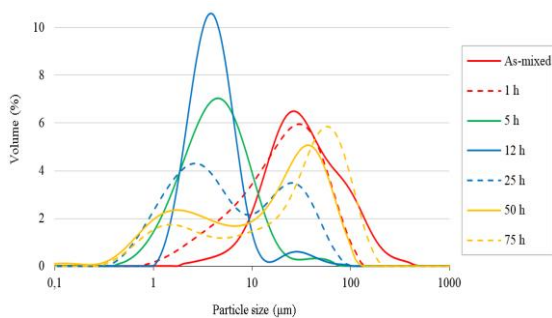


Fig. 1. Granulometric curves of as-mixed and mechanically alloyed $\text{Al}_{37}\text{Ti}_{63}$ powders for different milling times.

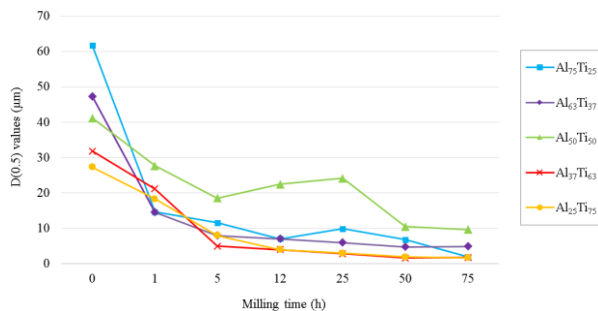


Fig. 2. $D(0.5)$ values of the different Al-Ti alloys milled for different times.

Scanning Electron Microscopy (SEM). Detailed SEM observations were performed to determine the powders morphology and particle size during the different stages of the MA process. Fig. 3 and 4 display the SEM micrographs of ball-milled $\text{Al}_{37}\text{Ti}_{63}$ powders after selected times. Milling for 1 hour makes the particles to have a very irregular lamellar form (Fig. 3a). After 5 hours of milling (Fig. 3b), particles acquire a more equiaxed geometry and a more homogeneous composition, and their size, as shown by granulometric analyses, is considerably reduced. After 25 hours of milling, the particle size is reduced to about $2\ \mu\text{m}$, but there is a clear powder agglomeration, related to the formation of the aforementioned second peak in the granulometric curves, with particles of up to $200\ \mu\text{m}$, as shown in Fig 3c.

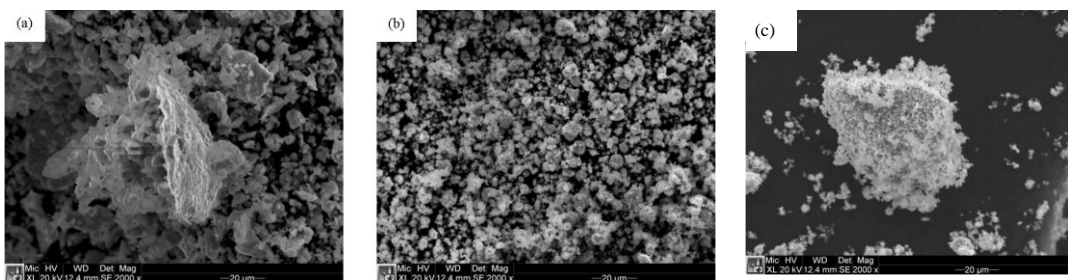


Fig. 3. SEM image of $\text{Al}_{37}\text{Ti}_{63}$ powders milled for (a) 1 h, (b) 5 h and (c) 25 h.

X-Ray Diffraction (XRD). Different behaviors of the $\text{Al}_{37}\text{Ti}_{63}$, $\text{Al}_{50}\text{Ti}_{50}$, $\text{Al}_{63}\text{Ti}_{37}$ and $\text{Al}_{75}\text{Ti}_{25}$ alloys using X-rays diffraction are shown in Fig. 4-7. $\text{Al}_{25}\text{Ti}_{75}$ alloy has a very similar behavior to $\text{Al}_{37}\text{Ti}_{63}$ alloy. For all Al-Ti alloys, comparing the unmilled powder mixture (Fig. 4a-7a) with powder milled for 1 hour (Fig. 4b-7b), the crystalline peaks start broadening due to the decrease of crystallite size and the increase in atomic level strain. Also, the intensities of the elemental crystalline diffraction peaks are reduced. After 5 hours for $\text{Al}_{25}\text{Ti}_{75}$ and $\text{Al}_{37}\text{Ti}_{63}$ (Fig. 4c), 12 h for $\text{Al}_{50}\text{Ti}_{50}$ (Fig. 5d) and 25 h for $\text{Al}_{63}\text{Ti}_{37}$ (Fig. 6e), diffractions lead to a pattern with only a broad diffuse maximum at $2\Theta = 39^\circ$, indicating that the elemental powder mixture has mainly transformed to a nanocrystalline phase or an amorphous one. Diffraction patterns of powders milled for longer times (except $\text{Al}_{50}\text{Ti}_{50}$) correspond to two broad peaks with low intensity at $2\Theta = 36^\circ$ and 42° , which might correspond to the formation of some intermetallic compound. Otherwise, the $\text{Al}_{50}\text{Ti}_{50}$ alloy maintains the broad peak at $2\Theta = 39^\circ$ until 75 hours of milling.

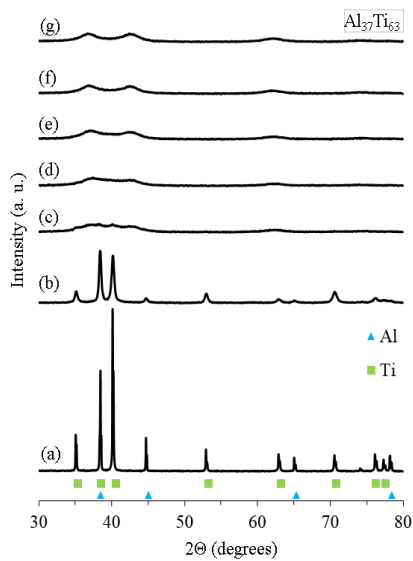


Fig. 4. XRD patterns of $\text{Al}_{37}\text{Ti}_{63}$ (a) mixture, and alloys milled for (b) 1 h, (c) 5 h, (d) 12 h, (e) 25 h, (f) 50 h and (g) 75 h.

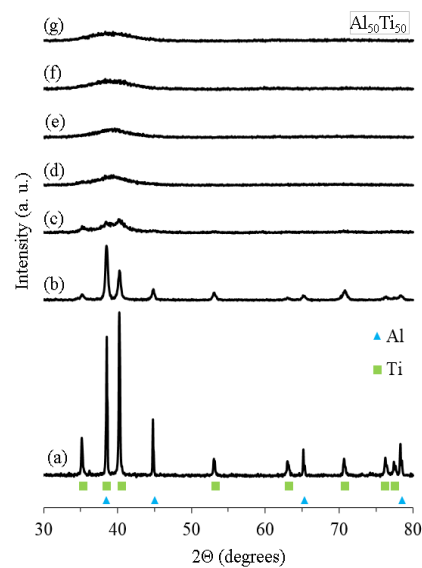


Fig. 5. XRD patterns of $\text{Al}_{50}\text{Ti}_{50}$ (a) mixture, and alloys milled for (b) 1 h, (c) 5 h, (d) 12 h, (e) 25 h, (f) 50 h and (g) 75 h.

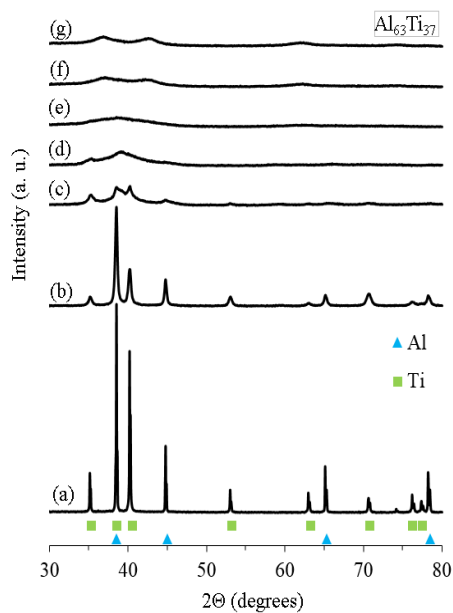


Fig. 6. XRD patterns of $\text{Al}_{63}\text{Ti}_{37}$ (a) mixture, and alloys milled for (b) 1 h, (c) 5 h, (d) 12 h, (e) 25 h, (f) 50 h and (g) 75 h.

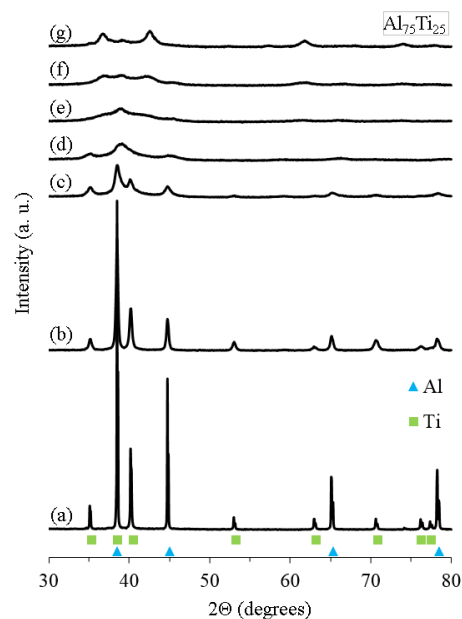


Fig. 7. XRD patterns of $\text{Al}_{75}\text{Ti}_{25}$ (a) mixture, and alloys milled for (b) 1 h, (c) 5 h, (d) 12 h, (e) 25 h, (f) 50 h and (g) 75 h.

Transmission Electron Microscopy (TEM). To demonstrate the structural evolution of the powders, sample $\text{Al}_{50}\text{Ti}_{50}$ was investigated by TEM. Diffraction pattern of sample milled for 50 hours (Fig. 8) shows typical features of an amorphous phase and no crystallites were detected anywhere in the specimen, thus supporting the XRD results.

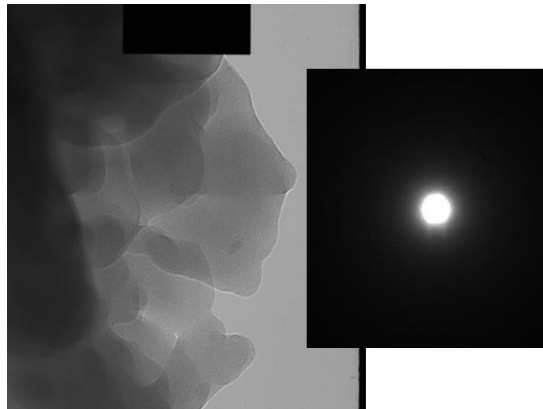


Fig. 8. TEM image and selected area diffraction pattern of $\text{Al}_{50}\text{Ti}_{50}$ milled for 50 h.

Differential Scanning Calorimetry (DSC). The thermal evolution by DSC of the Al-Ti powders milled for 50 hours can be observed in Fig. 9. The DSC curves for $\text{Al}_{25}\text{Ti}_{75}$, $\text{Al}_{37}\text{Ti}_{63}$, $\text{Al}_{63}\text{Ti}_{37}$ and $\text{Al}_{75}\text{Ti}_{25}$ alloys show an exothermic peak beginning at around 400 °C and ending at about 650 °C. The formation of intermediate crystalline phases from the solid solution of Al(Ti) or Ti(Al), partially formed for this milling time, could be responsible for the appearance of these exothermic peaks. For the $\text{Al}_{50}\text{Ti}_{50}$ alloy, the endothermic peak at about 480 °C marks the existence of a supercooled liquid region, and the exothermic peak at about 530 °C corresponds to the crystallization of the amorphous phase.

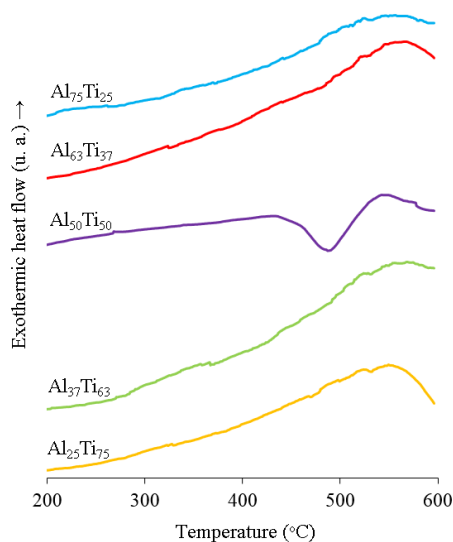


Fig. 9. DSC of the different Al-Ti powders milled for 50 h.

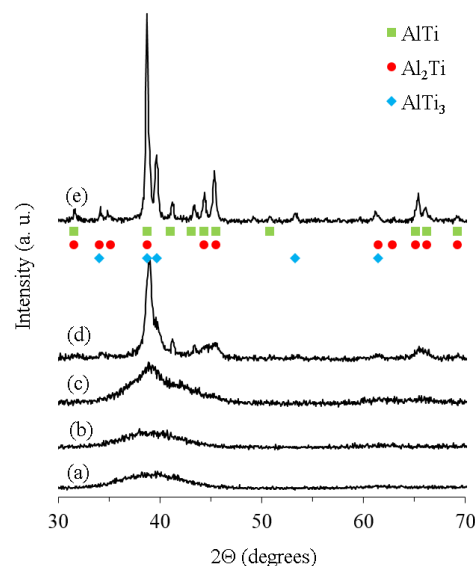


Fig. 10. XRD patterns of $\text{Al}_{50}\text{Ti}_{50}$ powder (a) milled for 50 h, and after heating up to (b) 300° C, (c) 500° C, (d) 650° C and (e) 850° C.

X-Ray Diffraction after Heat Treatment. Fig. 10 shows X-ray diffraction patterns of powders milled for 50 hours and subsequently heat treated at various temperatures. From 500 °C (Fig. 10c), an increase in the intensity around the peak corresponding to the presence of the amorphous phase is revealed. From 650 °C (Fig. 10d) the material crystallizes more clearly, resulting in the intermetallic compounds AlTi, Al_2Ti and AlTi_3 . Following the heat treatment until 850 °C (Fig. 10e)

emphasizes the presence of the crystalline phases, showing the main peak and several secondary peaks.

Conclusions

The formation of an amorphous phase by mechanical alloying using a high energy attritor ball mill was found for $\text{Al}_{25}\text{Ti}_{75}$, $\text{Al}_{37}\text{Ti}_{63}$, $\text{Al}_{50}\text{Ti}_{50}$ and $\text{Al}_{63}\text{Ti}_{37}$ alloys. The most stable amorphous phase has been obtained for $\text{Al}_{50}\text{Ti}_{50}$ alloy with a milling time between 50 and 75 hours. This amorphous phase is stable up to 300 °C. The crystallization of amorphous phase occurs at about 500 °C resulting in intermetallic compounds AlTi , Al_2Ti and AlTi_3 .

Acknowledgments

Financial support of the Ministerio de Economía y Competitividad (Spain) and Feder (EU) through the research project DPI2015-69550-C2-1-P is gratefully acknowledged.

References

- [1] W. Klement, R. H. Wilens, P. Duwez, *Nature*, **187** (1960) 869-870.
- [2] A. Inoue, *Progress in Materials Science*, **43** (1998) 365-520.
- [3] C. Suryanarayana, *Progress in Materials Science*, **46** (2001) 1-184.
- [4] F. Appel, U. Brossmann, U. Christoph, S. Eggert, P. Janschek, U. Lorenz, J. Müllauer, M. Oehring, J. D. Paul, *Adv. Eng. Mater.*, **2** (2000) 699–720.
- [5] J. Aguilar, A. Schievenbusch, O. K ättilitz, *Intermetallics*, **19** (2011) 757–761.
- [6] P.C. Priarone, S. Rizzuti, L. Settineri, G. Vergnano, *J. Mater. Process. Technol.*, **212** (2012) 2619–2628.
- [7] T. Tetsui, T. Kobayashi, T. Mori, T. Kishimoto, H. Harada, *Mater. Trans.*, **51** (2010) 1656.
- [8] J. Lapin, Z. Gabalcová *Intermetallics*, **19** (2011) 797–804.
- [9] W. Guo, A. Iasonna, M. Magini, S. Martelli, F. Padella, *J. Mater. Sci.*, **29** (1994) 2436-2444.
- [10] B. S. Murty, M. D. Naik, S. Ranganathan, M. Mohan Rao, *Mater. Forum*, **16** (1992) 19-26.
- [11] L. Schultz, *Mater. Sci. and Eng.*, **97** (1988) 15-23.
- [12] W. Guo, S. Martelli, N. Burgio, M. Magini, F. Padella, E. Paradiso, I. Soletta, *J. Mater. Sci.*, **26** (1991) 6190-6196.
- [13] M. Sherif El-Eskandarany, *J. Alloy Compd*, **234** (1996) 67-82.
- [14] S.I. Talabi, S. Oluropo, A. Funsho, I. Na'Allah, S. Abdulkareem, *International Journal of Metals*, Volume 2013 (2013), Article ID 127106.
- [15] J.B. Al-Dabbagh, R. Mohd, M. Ishak, S. Aisyah, *Int. J. Nanoelectronics and Materials*, **8** (2015) 23-32.